The Evolution of Vibration Sonoelastography

Kevin J. Parker*

Department of Electrical and Computer Engineering, University of Rochester, Rochester, NY 14627 USA

Abstract: The field of imaging the elastic properties of tissue has grown to an impressive variety of techniques and applications, some of which are currently in clinical trials. This review focuses on the specific role of vibration sonoelastography, beginning with the first images of tissue "hardness", through the development of real time scanning techniques, 3D reconstructions, and applications to major disease categories, especially the detection of prostate cancer.

Keywords: Vibration elastography, shear waves, tissue stiffness, hardness, biomechanics, imaging elastic properties of tissue, sinusoidal shear waves, diagnosis, cancer detection.

INTRODUCTION

The availability of Doppler ultrasound devices led to a number of studies of tissue motion and abnormalities in the 1970s and 1980s. Out of this background came vibration sonoelastography, where vibrational shear waves (typically between 50 and 1000 Hz continuous wave) are excited within tissue and the resulting vibrations are imaged and displayed using Doppler displacement or phase estimators. Analysis of the vibration patterns yields either images of relative tissue hardness or quantitative maps of elastic modulus, depending on the particular approach. The organization of the paper is as follows: first, we review some of the landmark studies of tissue motion leading up to the development of vibration elastography. Then the first known image of relative hardness is discussed in context, along with the early progression of vibration sonoelastography from 1987 into the early 1990s. The major developments up to the current era are categorized in sections covering Theory, Clinical Applications, 3D Prostate Imaging, and Biomechanics, with a particular focus on the results from the University of Rochester. Vibration phase gradient techniques and crawling waves are also covered. The development of these approaches over 20 years has provided a fertile ground for investigating tissues, organs and lesions in ways that were not previously possible. Other approaches that employ sinusoidal vibrations are reviewed elsewhere in this special issue [1, 2, 3, 4, 5].

1. BACKGROUND STUDIES OF TISSUE PROPERTIES FROM MOTION

A landmark study of the behavior of the human body when subjected to mechanical vibrations or sound fields was published by Oestreicher and colleagues [6, 7]. Photography and a strobe light were used to record vibration waves on the skin. Resultant surface wave propagation patterns gave wavelength and wave speed data, which led to the formulation of a theory to correlate increased frequency with increased tissue impedance. From experimental data, the shear modulus was calculated.

A signal processing technique used to measure small liver tissue displacements caused by vessel diameter differences during aortic pulsation was presented by Wilson and Robinson [8]. Assuming that the tissue followed points of constant phase, they obtained radio frequency (RF) M-mode signals and calculated the tissue motion velocity from the trajectory of a constant phase point. A coarse estimate of displacement was achieved by integrating velocity over time.

The correlation coefficient between consecutive A-scans was used by Dickinson and Hill [9] to measure tissue motion frequency and amplitude. In order to measure the changes of the interrogated region between two consecutive A-scans, a correlation parameter was established. The correlation parameter, which is unity for stationary tissue, decreases monotonically as tissue motion increases. Tristam *et al.* [10, 11] took this approach further to investigate the varied responses of normal liver and cancerous liver to cardiac movement. Various features on the correlation curves were found to distinguish normal liver from that with tumor. Livers with tumor were found to have lower maximum values, fewer peaks, and greater regularity. Modifying the correlation technique to measure tissue motion, De Jung *et al.* [12] found the maximum cross-correlation using an interpolation algorithm.

Pulmonary maturity and assessment of normal pulmonary development can be indicated by fetal lung elasticity. An attempt to qualitatively determine the stiffness of fetal lung was made by Birnholz and Farrell [13]. This was done by evaluating ultrasound B-scans, which indicate lung compression due to cardiac pulsations. They proposed that soft lung tissue compresses (with maximal deformation immediately adjacent to the heart) while stiff lung tissue exhibits no regional deformation (it transmits cardiac pulsations moving as a block). More quantitative approximations were achieved by Adler *et al.* [14, 15]. They were able to estimate <r>, a parameter that characterizes the range of transmitted cardiac motion in fetal lung, by applying correlation techniques to digitized M-mode images. In actuality, the parameter is the spatially and temporally-averaged systolic to diastolic deformation per unit epicardial displacement.

Induced quasistatic compression was investigated by Eisensher *et al.* [16]. This was accomplished by applying a 1.5-Hz vibration source to liver and breast tissue and using

*Address correspondence to this author at the Department of Electrical and Computer Engineering, University of Rochester, Rochester, NY 14627 USA; Tel: (585)275-3294; Fax (585)273-4919;
E-mail: kevin.parker@rochester.edu

1875-6603/11 $58.00+.00

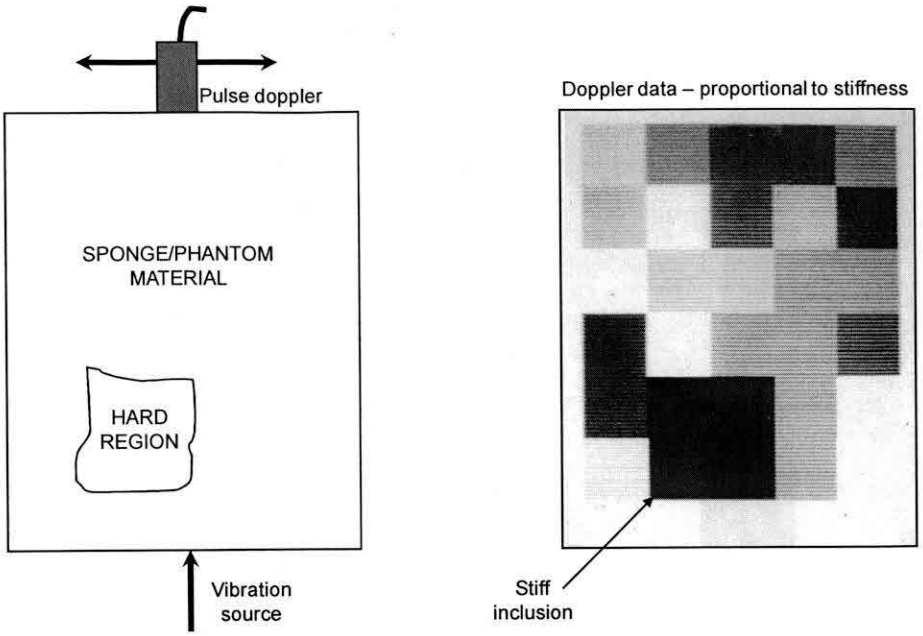

Fig. (1). Original imaging data and schematic of the first known image of relative stiffness, derived from Doppler data in a phantom with applied vibration. The original image was published in 1987 and 1988 [21, 22].

M-mode ultrasound. It was found that benign lesions had characteristically sinusoidal quasistatic compression response, while malignant tumors tended to have a more nonlinear (flat) response.

One of the first quantitative measurements of tissue elasticity using gated pulsed Doppler was reported by Krouskop *et al.* [17]. Assuming isotropy and incompressibility, the equations relating tissue properties and tissue movements were reduced to linear forms. Measuring tissue peak displacements and their gradients becomes the final reductive solution to finding tissue elasticity. They measured actual tissue motion at various points of interest under external vibration created by one A-line pulsed Doppler instrument. A possible measurement of tissue stiffness in a very small region (*i.e.,* 0.5 X 0.5 mm) was suggested. This paper is noteworthy in that it presages, with local Doppler vectors and external vibration, MRE and vibration sonoelastography.

In certain cases, the Doppler spectrum produced by the scattered ultrasound signal from a vibrating target can be similar to a pure-tone frequency modulation in that it has symmetric side harmonics in the area of the carrier frequency. The harmonic spacing is the same as the target vibrating frequency. The harmonic amplitudes are given by consecutive Bessel functions of the first kind. The expression for the signal [18] is:

$$s_r(t) = A\sum_{-\infty}^{\infty} J_n(\beta)\cos[\omega_0 t + n(\omega_L t + \phi)]$$

In this function, β is proportional to the vibrating amplitude of the tissue. The ultrasound signal's angular frequency is represented by ω_0, the target vibration's angular frequency is represented by ω_L and the vibration phase is represented by ϕ.

Using Doppler ultrasound to examine the abnormal oscillation of heart valves, Holen *et al.* [19] detected this characteristic Bessel-band Doppler spectrum. By counting the number of significant harmonics (as an estimation of the frequency modulated bandwidth), the amplitude of the vibration was estimated.

The Doppler ultrasound response to a low-frequency sound field in the auditory organs of fish was examined by Cox and Rogers [20]. By analyzing the ratio of the carrier to the first side band of the Doppler spectrum, the amplitude of the hearing organ's vibration was discovered.

2. VIBRATION ELASTOGRAPHY IMAGING

2.1. Vibration Amplitude Sonoelastography; Early Work

In 1987, Lerner and Parker presented early work on vibration amplitude sonoelastography [21, 22]. Vibration amplitude sonoelastography entails the application of a continuous low-frequency vibration (50-1000 Hz) to excite internal shear waves within the tissue of interest. A disruption in the normal vibration patterns will result if a stiff inhomogeneity is present in soft tissue surroundings. A real-time vibration image can be created by Doppler detection algorithms. Modal patterns can be created in certain organs with regular boundaries. The shear wave speed of sound in the tissue of these organs can be ascertained with the information revealed by these patterns [23].

Fig. (**1**) reproduces the first vibration amplitude sonoelastography image [21, 22]. The vibration within a sponge and saline phantom containing a harder area (the dark region) is depicted by this crude image. Range-gated Doppler was used to calculate the vibration amplitude of the interior of the phantom as it was vibrated from below. By 1990, a modified color Doppler instrument was used by the University of Rochester group to create real-time vibration amplitude sonoelastography images. In these images, vibration above a certain threshold (in the 2 micron range) produced a saturated color (Fig (**2**)).

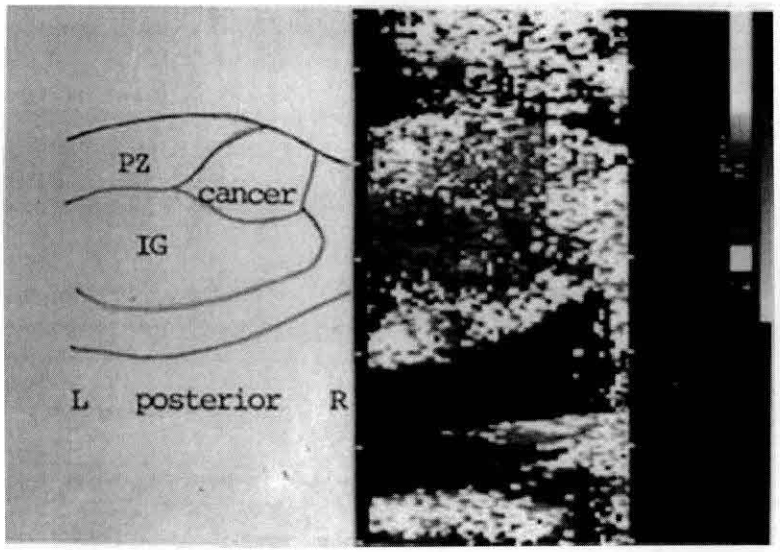

Fig. (2). A representative first generation image of vibration sonoelastography, circa 1990. Doppler spectral variance is employed as an estimator of vibration in the 1-10 micron range and displayed over the B-scan images. No color implies low vibrations below threshold. Shown is the fill-in of vibration within a whole prostate, with a growing cancerous region indicated by the deficit of color within the peripheral zone. Courtesy of Dr. R. M. Lerner.

Tissue elastic constant measurement results, vibration amplitude sonoelastography finite element modeling results, and phantom and *ex-vivo* tissue results were reported [24, 25, 26]. Thus, by the end of 1990, the working elements of vibration elastography (sonoelastography and sonoelasticity were other names used at the time) were in place, including real-time imaging techniques and stress-strain analysis of tissues such as prostate, with finite element models and experimental images demonstrating conclusively that small regions of elevated Young's modulus could be imaged and detected using conventional Doppler imaging scanners.

2.2. Theory

Along with the useful finite element approach of [25, 26], there were important theoretical questions to be answered by analytical or numerical techniques. How did vibration fields behave in the presence of elastic inhomogeneities? What is the image contrast of lesions in a vibration field, and how does the contrast depend on the choice of parameters? How do we optimally detect sinusoidal vibration patterns and image them using Doppler or related techniques? These important issues were addressed in a series of papers through the 1990s. One foundational result was published in 1992 under the title: "Sonoelasticity of Organs, Shear Waves Ring a Bell" [23]. This paper demonstrated experimental proofs that vibrational eigenmodes could in fact be created in whole organs including the liver and kidneys where extended surfaces create reflections of sinusoidal steady state shear waves. Lesions would produce a localized perturbation of the eigenmode pattern, and the background Young's modulus could be calculated from the patterns at discrete eigenfrequencies. Thus, both quantititative and relative imaging contrast detection tasks could be completed with vibration elastography in a clinical setting, *in-vivo*, by 1992. A later review of eigenmodes and a strategy for using multiple frequencies simultaneously (called "chords") was given in [27].

In 1994 a vibration amplitude analytical model was created [28]. This model used a sonoelastic Born approximation to solve the wave equations in an inhomogeneous, isotropic medium. The total wave field inside the medium can be expressed as:

$$\Phi_{total} = \Phi_i + \Phi_s$$

where Φ_i is the homogeneous or incident field, and Φ_s is the field scattered by the inhomogeneity. They satisfy, respectively:

$$(\nabla^2 + k)\Phi_i = ()$$

$$(\nabla^2 + k)\Phi_s = \delta(x)$$

where $\delta(x)$ is a function of the properties of inhomogeneity. The theory accurately describes how a hard or a soft lesion appear as disturbances in a vibration pattern. Fig. (**3**) summarizes the theoretical and experimental trends.

Signal processing estimators were also developed in the study of vibration amplitude sonoelastography. A method to estimate β from the spectral spread was suggested by Huang *et al.* [29], where β is proportional to the vibration amplitude of the target. They found a simple correlation between β and the Doppler spectral spread σ_ω:

$$\beta = \sqrt{2}(\sigma_\omega / \omega_L).$$

where ω_L is the vibration frequency of the vibrating target. This is an uncomplicated but very useful property of the Bessel Doppler function. The effect of noise, sampling and nonlinearity on the estimation was also considered. In their later work, they studied real-time estimators of vibration amplitude, phase, and frequency that could be used for a variety of vibration sonoelastography techniques [30].

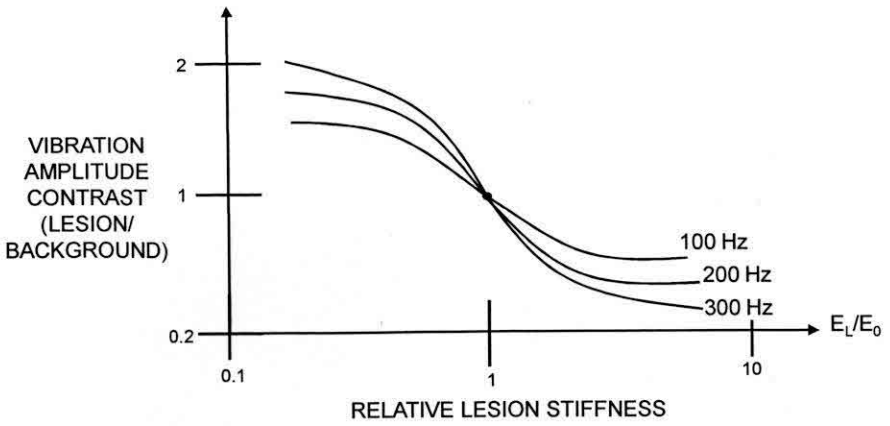

Fig. (3). Theoretical results of the contrast of vibration sonoelastography for soft or hard lesions in a background medium. The image contrast increases with both increasing frequency and with increasing size of the lesion.

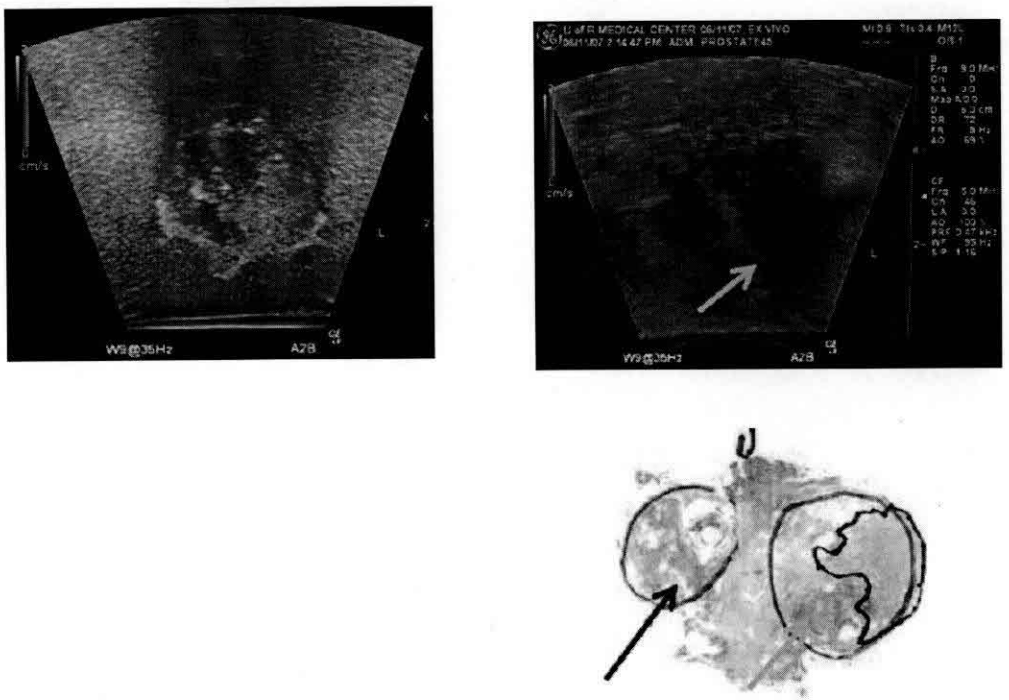

Fig. (4). Prostate B-scan, sonelastography and corresponding pathology. Blue circles on the pathology slides indicate BPH, black outline indicates cancer. The sono image shows a lower contrast deficit from the BPH (red arrow) and a higher contrast deficit, or dark region, from the cancer on the right border.

Finally, an overall theoretical approach that places vibration sonoelastography on a biomechanical spectrum with other techniques including compression elastography, MRE, and the use of impulsive radiation force excitations, is found in "A Unified View of Imaging the Elastic Properties of Tissues" [31].

2.3. Clinical Applications

By implementing various time and frequency estimators, this technique became a real-time diagnostic tool with applications for both deep and superficial organs. The liver, kidney, prostate and breast were imaged using vibration sonoelastography to characterize typical patterns and frequency ranges [23, 32, 33, 34]. Vibration amplitude sonoelastography was shown to have better sensitivity and predictive value than B-scan imaging alone in a 1994 study [33] of *ex-vivo* prostate cancer.

A more recent example of sonoelasticity imaging of a whole prostate surgery specimen is given in Fig. (**4**).

Muscle tissue was studied to demonstrate the relationship between Young's modulus of *in-vivo* muscle and applied load or exercise regimens [35, 36, 37, 38]. An unusual application of sonoelasticity is the measurement of intra-ocular pressure to test for glaucoma, via the resonance of the human eye *in-vivo* [39].

Another important application of elastography imaging is the precise delineation of thermal lesions produced intentionally by either microwaves, RF or HIFU. A series of pig liver lesions created by multiple methods were imaged by

sonoelastography and a high correlation was found between the lesion dimensions found by imaging and later measurements from gross pathology [40, 41], both *in-vivo* and *ex-vivo*.

2.4. Three-Dimensional Prostate Cancer Detection

Given the high incidence of prostate cancer in older males, and the poor sensitivity of conventional imaging modalities for detecting low contrast cancers of the prostate, there is a pressing need for improved imaging, detection and biopsy guidance. Vibration elastography appeared to be promising for prostate cancer detection from the earliest studies [32, 33]. However, the most rigorous approach would require 3D imaging of the prostate in B-scan - in sonoelastography - and for a gold standard, in sequential pathology slices demarcated by a pathologist for cancer, BPH (benign prostatic hyperplasia), and other abnormalities. We employed GE scanners with special Doppler Variance maps for imaging the vibration fields, along with an embedded 3D position sensor to recreate the images in both *in-vivo* scans and *ex-vivo* following radical prostatectomy. Special co-registration techniques were developed to fuse the ultrasound and pathology images. This requires careful consideration due to the shrinkage and warping of the tissue during preparation for obtaining sequential pathology slices (Fig (**5**)).

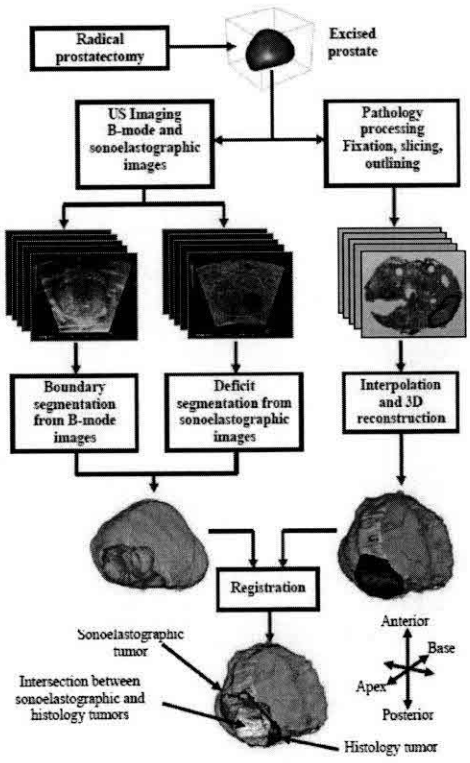

Fig. (5). 3D prostate imaging protocol. Courtesy of Prof. B. Castaneda.

The results demonstrated an increase in sensitivity and specificity on cancer detection into the mid 80% level [27, 42, 43, 44, 45, 46, 47, 48]. This represents an advance over conventional radiology and ultrasound, and increases the ability to localize suspicious regions for biopsy. However, the results at this point are not accurate enough to eliminate biopsy, and the role of BPH in creating false positives requires further study. There are a number of improvements in techniques that could lead to a further increase in sensitivity and specificity of sonoelastography for prostate cancer.

2.5. Vibration Phase Gradient Sonoelastography

In parallel to the early work at the University of Rochester, a vibration phase gradient approach to sonoelastography was developed by Professor Sato in the late 1980s at the University of Tokyo [49]. The amplitude and the phase of low-frequency wave propagation inside tissue were mapped. Wave propagation velocity and dispersion properties– which are directly linked to the elastic and viscous characteristics of tissue - were derived from this mapping.

The phase modulated (PM) Doppler spectrum of the signal returned from sinusoidally-oscillating objects approximates that of a pure-tone frequency modulation (FM) process. This similarity indicates that the tissue vibration amplitude and phase of tissue motion may be estimated from the ratios of adjacent harmonics.

The amplitude ratio between contiguous Bessel bands of the spectral signal is:

$$A_{i+1} / A_i = |J_{i+1}(\beta) / J_i(\beta)|$$

where A_i is the amplitude at the ith harmonic, β is the unknown amplitude of vibration in the tissue, and $J_i(\cdot)$ is an ith order Bessel function. β can be estimated from the experimental data if A_{i+1} / A_i, is calculated as a function of β beforehand. The phase of the vibration was calculated from the quadrature signals.

The display of wave propagation as a moving image is permitted by constructing phase and amplitude maps (Fig. (**6**)) as a function of time.

The use of a minimum squared error algorithm to estimate the direction of wave propagation and to calculate phase and amplitude gradients in this direction allows images of amplitude and phase to be computed offline. Assuming that the shear viscosity effect is negligible at low frequencies, preliminary *in vivo* results were demonstrated [49].

Sato's technique [49] was used and refined by Levinson [36]. A more general model of tissue viscoelasticity and a linear recursive filtering algorithm based on cubic B-spline functions were used. Levinson took the Fourier transform of the wave equation and derived the frequency domain displacement equation for a linear, homogeneous, isotropic viscoelastic material. From this, equations that relate the shear modulus of elasticity and viscosity to the wave number and the attenuation coefficient of the wave can be derived.

In 1995, Levinson *et al.* [36] conducted a series of experiments on the quadriceps muscle group in human thighs. It was assumed that shear waves predominate and that viscosity at low frequencies is negligible. Phase gradient images of the subjects' thighs under conditions of active muscle contraction enabled the calculation of Young's modulus of elasticity. The tension applied to the muscle was con-

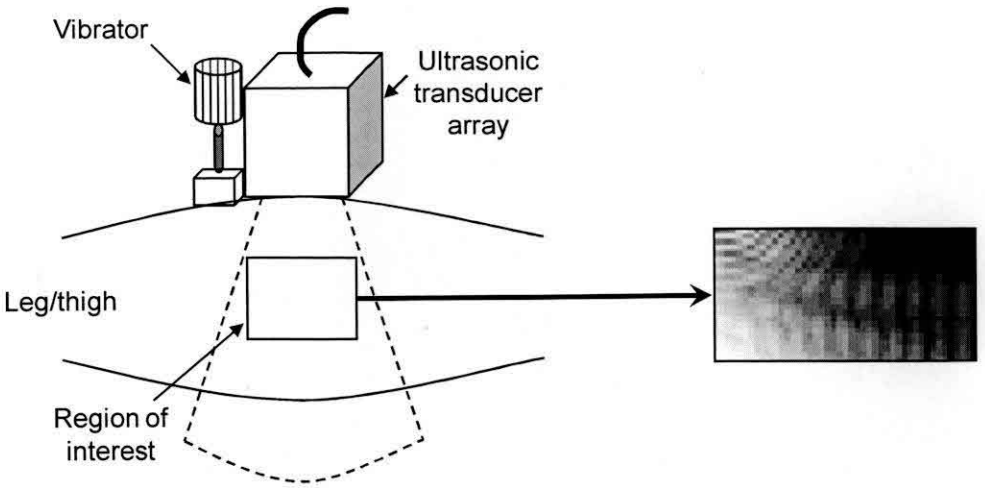

Fig. (6). A depiction of the system developed by Prof. Sato and colleagues at the University of Tokyo, including external vibration and an imaging array with signal processing for estimating the phase of the vibration in tissue. The rate of change of phase can be estimated to yield tissue hardness.

trolled using a pulley device. The measured vibration propagation speed and the calculated values of Young's modulus increased with the increasing degrees of contraction needed to counteract the applied load.

2.6. Crawling Waves

A fascinating extension of vibration sonoelastography is the use of an interference pattern formed by two parallel shear wave sources. The interference patterns reveal the underlying local elastic modulus of the tissue. The term "crawling waves" comes from the useful fact that by implementing a slight frequency or progressive phase difference between the two parallel sources, the interference pattern will move across the imaging plane at a speed controlled by the sources [50]. Thus, the crawling waves are readily visualized by conventional Doppler imaging scanners at typical Doppler frame rates; there is no need for ultrafast scanning. Other advantages of crawling waves include: the large region of interest excited between the two sources; most of the energy in the crawling waves is aligned in the Doppler (axial) direction, and a number of analysis or estimation schemes can be applied in a straightforward manner to derive the quantitative estimate of local shear wave velocity and Young's modulus. Crawling waves can also be implemented by a number of techniques including mechanical line sources, surface applicators, or radiation force excitations of parallel beams.

The use of crawling waves was first described in [50] by Wu *et al* at the University of Rochester. It was shown that crawling waves could be used to accurately derive the Young's modulus of materials and to delineate stiff inclusions [51, 52, 53, 54]. Estimators of shear wave speed and Young's modulus and the shear wave attenuation are derived in [55, 56, 57, 58]. Applications of crawling waves include the *ex-vivo* prostate [47, 59, 60], *in-vivo* muscle [38], and *ex-vivo* liver [53]. An example from *ex-vivo* prostate is given in Fig. (**7a**) and (**7b**).

Implementation into scanning probes can be accomplished by utilizing radiation force excitation along parallel beams [61, 62, 63].

2.7. Biomechanical Studies of Normal Tissue and Lesions

The entire field of imaging the elastic properties of tissues rests on the presumption that a meaningful elastic contrast exists between normal and diseased tissues, and this presumption is largely based on physical examination of tissues. Surprisingly, there is a paucity of data where elastography studies are compared against a rigorous gold standard of stress-strain measurements. However, utilizing the available tools of vibration elastography and crawling waves, a number of studies have been conducted that include reference measurements. A four-way agreement of i) shear wave time-of-flight measurements, ii) crawling wave measurements, iii) the Kelvin-Voight Fractional Derivative Model (KVFD), and iv) mechanical stress-strain measurement were described by Zhang *et al.* [53]. They demonstrated that the frequency dependent properties of viscoelastic tissues, including *ex-vivo* prostate and cancerous prostate tissues, liver, and others, could be derived from crawling wave experiments at discrete frequencies, or alternatively by mechanical stress strain measurements linked to the KVDF model of tissue viscoelasticity.

In other papers, utilizing these methods, the Rochester group measured an Elastic Contrast Ratio of 2.6/1 between cancerous and non-cancerous *ex-vivo* prostate tissues, at 150Hz [64]. Much higher contrast was found for thermally ablated liver tissue compared to normal liver tissue [40]. *In-vivo* skeletal muscle properties under different conditions were also determined using these methods [38]. The change in contrast between two dissimilar media as a function of frequency was demonstrated and explained in [65]. Overall, the combination of crawling waves measurements over a frequency range, combined with the KVDF model, has proven to be a useful imaging method for estimating the viscoelastic properties of tissues, *in-vivo* and ex-vivo. Furthermore, the crawling waves analysis closely corresponds to conventional mechanical measurements using stress and strain applied directly to cylindrical sections of tissue. Of course, the imaging techniques utilizing crawling waves do not require any excisions, and can be performed across the overlying skin and fat.

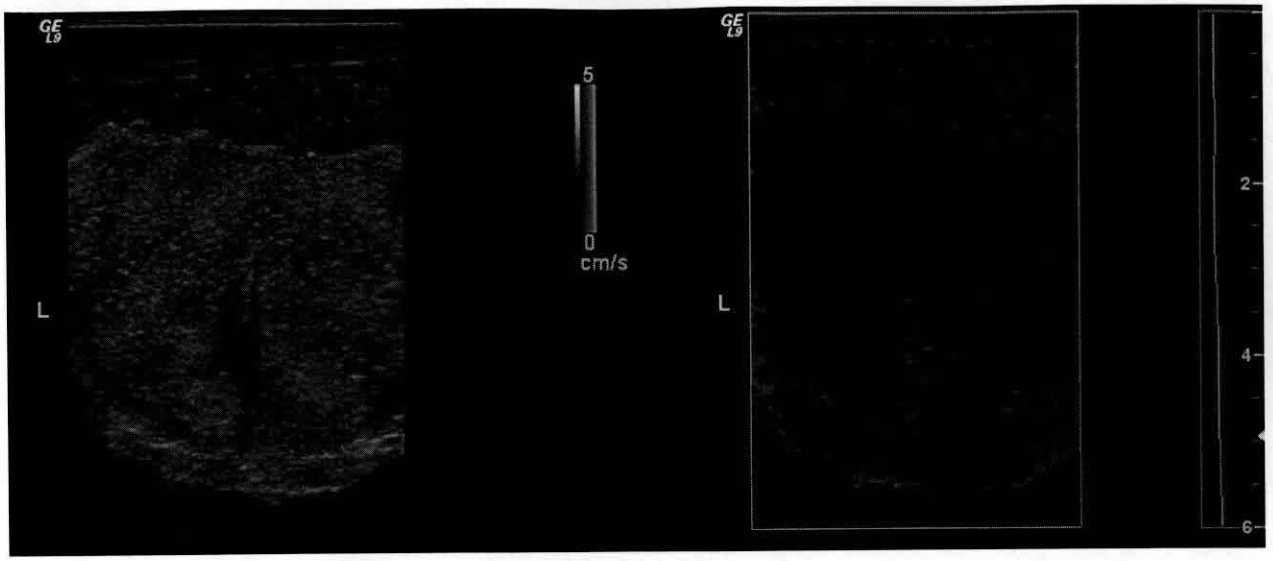

Fig. (7a).

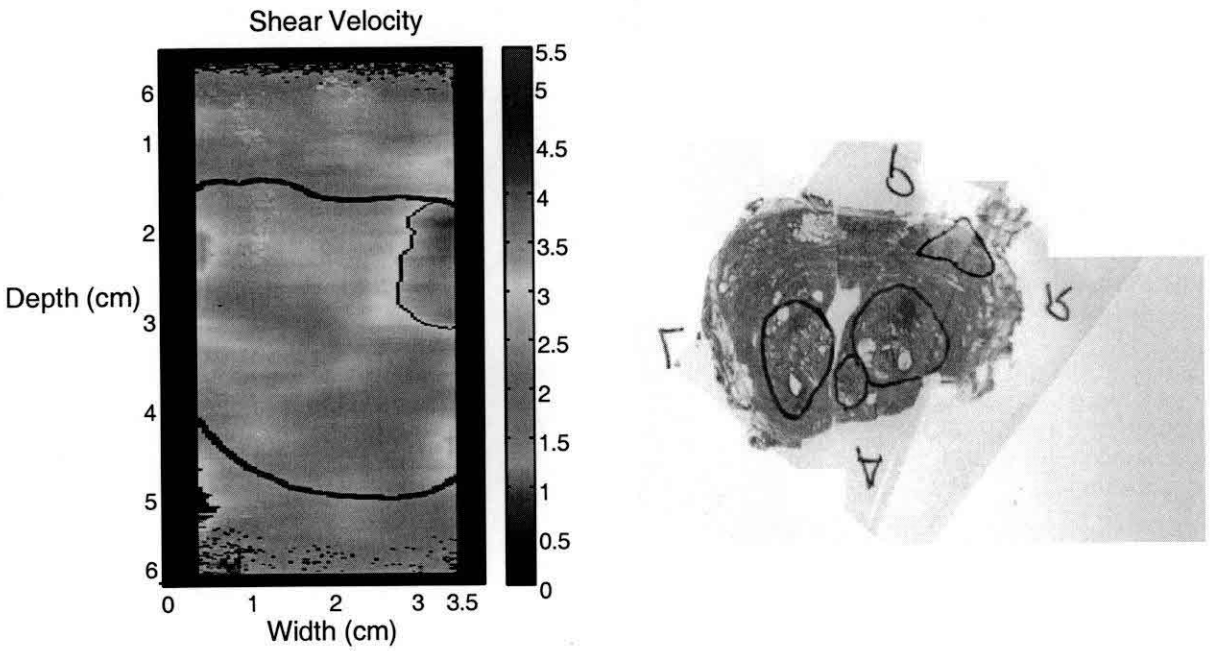

Fig. (7b).

Fig. (7a) and (7b). Crawling waves in the prostate. Fig. (**7a**), left: B-scan of whole excised prostate; Fig. (**7a**), right: crawling waves frame; Fig. (**7b**), right: pathology with labels: black=cancer and blue=BPH; Fig. (**7b**), left: quantitative estimates of shear velocity from crawling waves analysis, indicating the hard region as a red area (corresponding to the region with cancer). Estimates from an average of 3 frequencies are shown. All images are co-registered.

3. CONCLUSION

Vibration sonoelastography has seen steady developments across experimental, theoretical, clinical and biomechanical fronts for about 20 years. Benchmark developments at Rochester include the first known image of relative hardness of tissues presented in 1987, the development of real time Doppler vibration imaging techniques, the development of the Born-elastic theoretical formulation, applications to clinical problems, and the invention of crawling waves which provide another level of quantitative estimates while being compatible with conventional Doppler scanners. The early developments, along with Dr. Sato's work in Japan, set the stage for a remarkable proliferation of approaches and techniques to imaging the elastic properties of tissues [66].

ACKNOWLEDGEMENTS

The tremendous insights provided by Dr. Lerner, Dr. Rubens and co-authors of previous works are gratefully acknowledged. Support from and collaboration with superb colleagues at GE were essential parts of this research. The work presented was supported by NIH Grant 5R01AG02980-04.

REFERENCES

[1] Konofagou EE, Maleke C. Harmonic motion imaging (HMI) for tumor imaging and treatment monitoring – a review. CMIR 2011.

[2] Litwiller DV, Mariappan YK, Ehman RL. A review of magnetic resonance elastography. CMIR 2011.

[3] Urban MW, Chen S, Fatemi M. A review of shearwave dispersion ultrasound vibrometry (SDUV) and its applications. CMIR 2011.

[4] Sinkus R, Daire J-L, Vilgrain V, Van Beers BE. Elasticity imaging via MRI: basics, overcoming the Lamb wave limit, and clinical liver results. CMIR 2011.

[5] Urban MW, Alizad A., Aquino W, Greenleaf JF, Fatemi M. A review of vibro-acoustography and its applications in medicine. CMIR 2011.

[6] Oestreicher HL. Field and impedance of an oscillating sphere in a viscoelastic medium with and application to biophysics. J Acoust Soc Am 1951; 23: 707-14.

[7] Von Gierke HE, Oestreicher HL, Franke EK, Parrack HO, Von Wittern WW. Physics of vibrations in living tissues. J Appl Physiol 1952; 4: 886-900.

[8] Wilson LS, Robinson DE. Ultrasonic measurement of small displacements and deformations of tissue. Ultrason Imaging 1982; 4: 71-82.

[9] Dickinson RJ, Hill CR. Measurement of soft tissue motions using correlation between A-scans. Ultrasound Med Biol 1982; 8: 263-71.

[10] Tristam M, Barbosa DC, Cosgrove DO, Nassiri DK, Bamber JC, Hill CR. Ultrasonic study of *in vivo* kinetic characteristics of human tissues. Ultrasound Med Biol 1986; 12: 927-37.

[11] Tristam M, Barbosa DC, Cosgrove DO, Nassiri DK, Bamber JC, Hill CR. Application of Fourier analysis to clinical study of patterns of tissue movement. Ultrasound Med Biol 1988; 14: 695-707.

[12] De Jong PGM, Arts T, Hoeks APG, Reneman RS. Determination of tissue motion velocity by correlation interpolation of pulsed ultrasonic echo signals. Ultrason Imaging 1990; 12: 84-98.

[13] Birnholz JC, Farrell EE. Fetal lung development: Compressibility as a measure of maturity. Radiology 1985; 157: 495-8.

[14] Adler R, Rubin JM, Bland P, Carson P. Characterization of transmitted motion in fetal lung: Quantitative analysis. Med Phys 1989; 16: 333-7.

[15] Adler RS, Barbosa DC, Cosgrove DO, Nassiri DK, Bamber JC, Hill CR. Quantitative tissue motion analysis of digitized M-mode images: Gestational differences of fetal lung. Ultrasound Med Biol 1990; 16: 561-9.

[16] Eisensher A, Schweg-Toffer E, Pelletier G, Jacquemard G. La palpation échographique rythmée-echosismographie. J Radiol 1983; 64: 255-61.

[17] Krouskop TA, Dougherty DR, Levinson SF. A pulsed Doppler ultrasonic system for making noninvasive measurements of the mechanical properties of soft tissues. J Rehabil Res Biol 1987; 14: 1-8.

[18] Taylor KJ. Absolute measurement of acoustic particle velocity. J Acoust Soc Am 1976; 59: 691-4.

[19] Holen J, Waag RC, Gramiak R. Representation of rapidly oscillating structures on the Doppler display. Ultrasound Med Biol 1985; 11: 267-72.

[20] Cox M, Rogers PH. Automated noninvasive motion measurement of auditory organs in fish using ultrasound. J Vibrat Acoust Stress Reliabil Des 1987; 109: 55-59.

[21] Lerner RM, Parker KJ. Sonoelasticity images derived from ultrasound signals in mechanically vibrated targets. In: Tjissen J, ed. Proceedings of the Seventh European Communities Workshop. Nijmegen, The Netherlands, 1987.

[22] Lerner RM, Parker KJ, Holen J, Gramiak R, Waag RC. Sonoelasticity: Medical elasticity images derived from ultrasound signals in mechanically vibrated targets. Acoust Imaging 1988; 16: 317-27.

[23] Parker KJ, Lerner RM. Sonoelasticity of Organs: Shear waves ring a bell. J Ultrasound Med 1992; 11: 387-92.

[24] Parker KJ, Huang SR, Lerner RM, Lee F, Roach D. Elastic and ultrasonic properties of the prostate. IEEE Ultrasonics Symposium 1993.

[25] Lerner RM, Huang SR, Parker KJ. Sonoelasticity images derived from ultrasound signals in mechanically vibrated tissues. Ultrasound Med Biol 1990; 16: 231-39.

[26] Parker KJ, Huang SR, Musulin RA. Tissue response to mechanical vibrations for sonoelasticity imaging. Ultrasound Med Biol 1990; 16: 241-6.

[27] Taylor LS, Porter BC, Rubens DJ, Parker KJ. Three-dimensional sonoelastography: Principles and practices. Phys Med Biol 2000; 45: 1477-94.

[28] Gao L, Alam SK, Lerner RM, Parker KJ. Sonoelaticity imaging: Theory and experimental verification. J Acoust Soc Am 1995; 97: 3875-86.

[29] Huang SR, Lerner RM, Parker KJ. On estimating the amplitude of harmonic vibration from the Doppler spectrum of reflected signals. J Acoust Soc Am 1990; 88: 310-17.

[30] Huang SR, Lerner RM, Parker KJ. Time domain Doppler estimators of the amplitude of vibrating targets. J Acoust Soc Am 1992; 91: 965-74.

[31] Parker KJ, Taylor RS, Gracewski S, Rubens DJ. A unified view of imaging the elastic properties of tissue. J Acoust Soc Am 2005; 117: 2705-12.

[32] Lee F, Bronson JP, Lerner RM, Parker KJ, Huang SR, Roach DJ. Sonoelasticity imaging: Results in *in vitro* tissue specimens. Radiology 1991; 181: 237-9.

[33] Rubens DJ, Hadley MA, Alam SK, Gao L, Mayer RD, Parker KJ. Sonoelasticity imaging of prostate cancer: *In vitro* results. Radiology 1995; 195: 379-83.

[34] Zhang M, Nigwekar P, di Sant'Agnese *et al.* Quantitative characterization of viscoelastic properties of human prostate correlated with histology. Ultrasound Med Biol 2008; 34: 1033-42.

[35] Levinson SF. Ultrasound propagation in anisotropic soft tissues: The application of human skeletal muscle elasticity. J Biomech 1987; 20: 251-60.

[36] Levinson SF, Shinagawa M, Sato T. Sonoelastic determination of human skeletal muscle elasticity. J Biomech 1995; 28: 1145-54.

[37] Hoyt K, Castaneda B, Parker KJ. Muscle tissue characterization using quantitative sonoelastography: Preliminary results. Proceedings IEEE Ultrasonics Symposium 2007: 365-68.

[38] Hoyt K, Kneezel T, Castaneda B, Parker KJ. Quantitative sonoelastography for the *in vivo* assessment of skeletal muscle viscoelasticity. Phys Med Biol 2008; 53: 4063-80.

[39] Alam SK, Richards DW, Parker KJ. Detection of intraocular pressure change in the eye using sonoelastic Doppler ultrasound. Ultrasound Med Biol 1994; 20: 751-58

[40] Zhang M, Castaneda B, Christensen J *et al.* Real-time sonoelastography of hepatic thermal lesions in a swine model. Med Phys 2008; 35: 4132-41.

[41] Taylor LS, Zhang M, Strang G, Rubens DJ, Parker KJ. In-vitro imaging of thermal lesions using three-dimensional vibration sonoelastography. Proceedings Second International Symposium on Therapeutic Ultrasound 2002: 176-84.

[42] Porter B, Rubens DJ, Parker KJ. Soft tissue volume fusion of ultrasound and MRI. IEEE Trans Ultrason Ferroelectr Freq Control 1999; 46: cover image.

[43] Taylor LS, Porter B, Rubens DJ, Parker KJ. 3D sonoelastography for prostate tumor imaging. Intl ICSC Congress on Computational Intelligence: Methods and Applications. 1999; 468-472.

[44] Porter B, Parker KJ, Rubens DJ. Three-dimensional registration and fusion of ultrasound and MRI using major vessels as fiducial markers. IEEE Trans Med Imaging 2001; 20: 354-9.

[45] Taylor LS, Porter BC, Nadasdy G, *et al.* Three-dimensional registration of prostate images from histology and ultrasound. Ultrasound Med Biol 2004; 30: 161-8.

[46] Taylor LS, Rubens DJ, Porter BC, *et al.* Prostate cancer: three-dimensional sonoelastography for in vitro detection of prostate cancer. Radiology 2005; 237: 981-5.

[47] Hoyt K, Castenada B, Zhang M *et al.* Tissue elasticity properties as biomarkers for cancer in prostate. Cancer Biomarkers 2008; 4: 213-25.

[48] Castenada B, Hoyt M, Zhang M, *et al.* Prostate cancer detection based on three dimensional sonoelastography. Proceedings IEEE Ultrasonics Symposium 2007; 1353-6.

[49] Yamakoshi Y, Sato J, Sato T. Ultrasonic imaging of internal vibration of soft tissue under forced vibration. IEEE Trans Ultrason Ferroelectr Freq Control 1990; 37: 45-53.

[50] Wu Z, Taylor LS, Rubens DJ, Parker KJ. Sonoelastographic imaging of interference patterns for estimation of the shear velocity of homogeneous biomaterials. Phys Med Biol 2004; 49: 911-22.

[51] Wu Z. Shear wave interferometry and holography, an application of sonoelastography. Ph.D. dissertation, University of Rochester, 2005.

[52] Wu Z, Hoyt K, Rubens DJ, Parker KJ. Sonoelastographic imaging of interference patterns for estimation of shear velocity distribution in biomaterials. J Acoust Soc Am 2006; 120: 535-45.

[53] Zhang M, Castaneda B, Wu Z *et al.* Congruence of imaging estimators and mechanical measurements of viscoelastic properties of soft tissues. Ultrasound Med Biol 2007; 33: 1617-31.

[54] Wu Z, Taylor LS, Rubens DJ, Parker KJ. Shear wave focusing for three-dimensional sonoelastography. J Acoust Soc Am 2002; 111: 439-46.

[55] Hoyt K, Parker KJ, Rubens DJ. Real-time shear velocity using sonoelastographic techniques. Ultrasound Med Biol 2007; 33: 1086-97.

[56] McLaughlin J, Renzi D, Parker K, Wu Z. Shear wave speed recovery using moving interference patterns obtained in sonoelastography experiments. J Acoust Soc Am 2007; 121: 2438-46.

[57] Hoyt K, Castaneda B, Parker KJ. Feasibility of two-dimensional quantitative sonoelastographic imaging. Proceedings IEEE Ultrasonics Symposium 2007; 2032-5.

[58] Hoyt K, Castaneda B, Parker KJ. Two-dimensional sonoelastographic shear velocity imaging. Ultrasound Med Biol 2008; 34: 276-88.

[59] Hoyt K, Parker KJ, Rubens DJ. Sonoelastographic shear velocity imaging: experiments on tissue phantom and prostate. Proceedings IEEE Ultrasonics Symposium 2006; 1686-9.

[60] Castenada B, An L, Wu S *et al.* Prostate cancer detection using crawling wave sonoelastography. Proceedings SPIE Medical Imaging 2009: Ultrasonic Imaging and Signal Processing 2009; 726513-1 – 726513-10.

[61] Hah Z, Cho YT, An L *et al.* Methods for generating crawling waves with radiation force from ultrasonic beams. Proceedings AIUM, J Ultrasound Med 2010; 29: S1-14.

[62] Cho YT, Hah Z, An L *et al.* Theoretical investigation of strategies for generating crawling waves using focused beams. Proceedings AIUM, J Ultrasound Med 2010; 29: S1-14.

[63] An L, Rubens DJ, Strang J. Evaluation of crawling wave estimator bias on elastic contrast quantification. Proceedings AIUM, J Ultrasound Med 2010; 29: S1-14.

[64] Zhang M, Nigwekar P, di Sant'Agnese *et al.* Quantitative characterization of viscoelastic properties of human prostate correlated with histology. Ultrasound Med Biol 2008; 34: 1033-42.

[65] Taylor LS, Richards MS, Moskowitz AJ, Lerner AL, Rubens DJ, Parker KJ. Viscoelastic effects in sonoelastography. Proceedings IEEE Ultrasonics Symposium 2001.

[66] Parker KJ, Doyley MM, Rubens DJ. Imaging the elastic properties of tissue: the 20 year perspective. Phys Med Biol 2011; 56: R1-R29.

Received: May 04, 2010 Revised: August 24, 2010 Accepted: September 10, 2010